Mar. Biotechnol. 6, 541–551, 2004
DOI: 10.1007/s10126-004-3129-7

MARINE BIOTECHNOLOGY

Zonal Localization of Shell Matrix Proteins in Mantle of *Haliotis tuberculata* (Mollusca, Gastropoda)

Cécile Jolly, Sophie Berland, Christian Milet, Sandrine Borzeix, Evelyne Lopez, and Dominique Doumenc

Muséum National d'Histoire Naturelle, Département Milieux et Peuplements Aquatiques, Unité associée au CNRS, Biologie des Organismes Marins et Ecosystémes, 55 rue Buffon, 75231 Paris Cedex 05, France

Abstract: Organic matrix from molluscan shells has the potential to regulate calcium carbonate deposition and crystallization. Control of crystal growth thus seems to depend on control of matrix protein secretion or activation processes in the mantle cells, about which little is known. Biomineralization is a highly orchestrated biological process. The aim of this work was to provide information about the source of shell matrix macromolecule production, within the external epithelium of the mantle. An in vivo approach was chosen to describe the histologic changes in the outer epithelium and in blood sinus distribution, associated with mantle cells implicated in shell matrix production. Our results characterized a topographic and time-dependent zonation of matrix proteins involved in shell biomineralization in the mantle of *Haliotis*.

Key words: biomineralization, shell matrix, nacre, calcite, mantle, *Haliotis tuberculata*.

INTRODUCTION

Mollusk shell consists of mineral and organic matrix. The mineral part is calcium carbonate, which crystallizes under aragonite or calcite. The mineral is impregnated in biopolymers in extracellular space, within the extrapallial fluid, and the organic crystals are laid down in orderly arrays in intimate association with a matrix of organic macromolecules. It is believed that the growth and polymorphism observed in calcium carbonate crystal, such as aragonite and calcite in mollusk shell, is controlled by specialized organic matrix proteins secreted from the mantle epithelia (Belcher et al., 1996; Falini et al., 1996; Thompson et al., 2000).

Received November 11, 2003; accepted November 28, 2003; online publication March 9, 2005.

Corresponding author: Cécile Jolly; e-mail: Jolly.Cecile@ifm.uib.no

Epithelium is the first provider of the macromolecules involved in shell construction. The shell growth front is due to mantle epithelial cell activity (Saleuddin, 1976) in which organic macromolecules and inorganic ions are secreted into the extrapallial space between the mantle and the shell (Simkiss and Wilbur, 1987). After Crenshaw (1972) first characterized Ca-binding glycoprotein in the matrix extracted from the shell of *Merceneria merceneria,* subsequent studies focused on fractionation, purification, and characterization of the peptidic components of the matrix. Results were consistent with a highly acidic composition of the soluble matrix (Nakahara et al., 1981; Samata, 1990). The matrix proteins of the molluscan shell share a general capacity to bind calcium ions, and it has been clarified in vitro that the organic matrix is involved in the crystallization process (Falini et al., 1996). Matrix extracts may enhance or inhibit the crystal formation of calcium carbonate

(Belcher et al., 1996; Falini et al., 1996; Weiss et al., 2000). A central tenet of shell biomineralization is that the organic constituents including highly acidic proteins have an important role in the spatial and chemical control of crystal nucleation, growth, and microstructural fabrication (Weiner and Traub, 1984). Published data show that the range of variation of the organic matrix seems larger than that of the mineral part of the layers. There is growing information on the structure and composition of the macromolecules of the organic matrix and their possible role in crystallization control.

Thermal analysis of bivalvia shell shows that the organic matrix of aragonite layers differs from that of the prismatic layers (Kobayashi, 1973), and the protein pattern of the matrix partly supports this specificity. Some of the proteins of the shell matrix are unique to the calcitic composites or to the aragonitic layer. Sudo et al. (1997) reported 2 such proteins in the shell of *P. fucata*, in which MSI 60 is specific to the aragonitic layer and MSI 31 is specific to the calcitic layer.

Despite these recent advances in determining the biochemical basis of the biomineralization process and a growing number of studies on matrix protein characterization, there is still some controversy about the cells involved in matrix protein secretion. Relatively few studies have been done on Gastropoda, most of them on pulmonates (Saleuddin, 1975; Bielefeld et al., 1993).

The present study reflects a preliminary approach to investigating the protein synthesized in the mantle cells in *H. tuberculata* and localizing the cells involved in the secretion of the shell layers. Specific MSI 31 and MSI 60 antibodies were built from Sudo et al. (1997) data on sequences and processed for in situ immunocytochemistry in the mantle of *Haliotis*. Since there is seasonal variation in *Haliotis* growth (Clavier and Richard, 1985), we intended to address the results during and after the annual growing phase. Our work established a zonation in the external epithelium of the mantle and localized a cell population in which specific molecules are produced in a range of time related to the shell growth.

Materials and Methods

Haliotis tuberculata (Gasteropoda)

The specimens of *Haliotis* used in this study were kindly provided by the SMEL (Syndicat Mixte de l'Equipement du Littoral, Blainville sur mer, France). The animals were reared in seawater in temperature conditions ranging between 18° and 20°C without feeding limitation. Forty animals were used in this study. All of them belonged to an age class from 3 to 6 years (size range, 4–9 cm) and were not adult. This range was chosen to ensure a high growing capacity. Thirty abalone were collected from March to early May during the annual growing phase, and 10 were collected in late October during the resting period (Clavier and Richard, 1985).

The whole mantle margin that lines the shell from the mantle edge to the circum pedal cavity was dissected out using a razorblade, divided in 4 stereotactic quadrants, and immediately fixed in a 4% solution of paraformaldehyde fluid buffered in phosphate-buffered saline (PBS) adjusted to pH 7.6 for 12 hours at 4°C. The quadrants were drawn symmetrically to the long axis of the *Haliotis* shell: 2 anteriors (right and left), and 2 posteriors (right and left). The tissues were then rinsed in buffer, dehydrated, and prepared in butanol to be embedded in paraffin. Serial 6-µm sections were cut for subsequent studies.

Construction of Antibodies

Antibodies were constructed using the sequences of the framework proteins for the nacreous (MSI 60) and prismatic (MSI 31) layers of *P. fucata* reported by Sudo et al. (1997). Two sequences, about 15 amino acids in length each, were retained from the total sequences of the proteins for raising antibodies. Synthetic peptides were constructed as follows: SADGYDDYKKYGSV for anti–MSI 31–like and WGNNGNNKYDDDDCDE for anti–MSI 60–like antibody production.

These sequences were checked by screening the generalist sequence databases Swiss Prot and EMBL to avoid homologies with metabolic or other universal proteins. Sequence design fulfilled requirements of major importance for our purposes: potent immunogenecity, sequence specificity for either MSI 31 or MSI 60, and an important ratio of acidic amino acids, this criterion being a general feature of proteins, involved in biomineralization.

Sequence selection was accomplished using SYPEITHI software (Server of Molecular Expasy). The antibodies were raised in mice after the above-mentioned peptides were synthesized and coupled with hemocyanin by means of glutaraldehyde. Anti–MSI 31–like and anti–MSI 60–like antibodies used in this work were supplied by Eurogentec S.A. Seraing, Belgium.

Immunochemistry

After washing and blocking nonspecific protein attachment sites using normal rabbit serum (1:50) for 20 minutes at room temperature, sections were probed for peroxidase MSI 31–like and MSI 60–like immunolabeling. Hydrogen peroxide 3% was applied to the sections to avoid endogen peroxidase interference.

Immunoperoxidase labeling was revealed with the diaminobenzidine tetrachloride substrate in 0.03% hydrogen peroxide Tris-HCl (pH 7.6).

After the sections were rehydrated in ethanol concentration series, nonspecific antigenic sites were blocked with normal rabbit serum in PBS (1:50, pH 7.4) for 20 minutes at room temperature. Endogen peroxidase was blocked with hydrogen peroxide 3% diluted in PBS (1:2), for 30 minutes at room temperature. Sections were then incubated in diluted (1:2000) MSI 31 or MSI 60 antibody in PBS at 4°C overnight. They were rinsed in PBS, incubated in PBS + serum (1:100) diluted antimouse biotin conjugated at room temperature for 1 hour, then with extravidin-peroxidase complex at room temperature for 1 hour. Sections were then rinsed in distilled water and stained with toluidine blue. In the immunofluorescence procedure, sections were incubated overnight at 4°C in 1:2000 MSI 31 or MSI 60 antibody. They were rinsed in PBS and incubated in 1:100 Cy3 conjugated antibody from Sigma. Sections were dried at room temperature before observation.

The nuclei were visualized by DAPI (4', 6-diamidino-2-phenylindole) from Sigma for 1 hour in 1:100 PBS at room temperature. The slides were monitored using appropriate filters in a fluorescence microscope.

Controls

Three sets of control experiments were performed. In the first one, as a negative control, the immune serum was omitted. In the second, antibody specificity was checked by incubating the immune serum with the respective synthetic peptide for 1 hour prior to the immunocytochemical procedure. In the third, cross reactivity of the immune serum with the opposite synthetic peptide was checked by incubating MSI 31 antigen to the constructed anti–MSI 60 antibody, and vice versa, prior to the immunocytochemical procedure. The other steps of immunohistochemistry for control lots were processed as described above.

Results

General Structure of Mantle Edge

We focused on description of the external eipithelium because it was the only site where immunohistologic reactions occurred. At the shell edge, the mantle is made of a thin lamella of connective tissue covered by a single-cell-layered epithelium (Figure 1, a). The edge is marked by the periostracal groove lined by 2 folds in *Haliotis*. The groove separates the outer epithelium facing the shell from the circumpedal inner epithelium.

The connective tissue consists of muscular bundles and connective fibers. The muscular fibers organized in clusters beneath the outer epithelium caused the curvature of samples after fixation. The connective tissue also contains large blood sinuses, with hemocytes inside, sometimes in contact with the outer epithelial cells (Figure 1, c). Wandering hemocytes were also found within the connective tissue.

In the younger studied specimens (3 years old), the central region of the periostracal groove was lined with broad cells on the outer side, forming a pad. Local and DAPI staining indicated a bilayered nuclei arrangement in this region (Figure 1, b, d). On the inner side of the periostracal groove, cells were monolayered and contained numerous black (melanin) granules in their apical part, forming the peripheric black lining of the mantle edge. In the most proximal segment, the external epithelium formed sheets going toward the connective tissue and drawing a tubular zone facing the periostracal groove. This area was observed to be more or less developed according to the age of the specimens. Younger specimens showed a well-developed tubular zone. Inward, the external epithelium was monolayered and appeared folded in its proximal portion, then became more linear.

Immunohistologic Results

Ten specimens were collected in autumn, the low growing period. Neither MSI 31–nor MSI 60–like protein immunohistologic labeling was detected in the samples. Labeling following the immunohistologic procedure was only observed in the spring specimens and exclusively in the anterior right quadrant of the mantle. No immune reaction occurred in the other quadrants. Among the 30 specimens collected in spring, 23 were positive for MSI 31–like and MSI 60–like protein labeling in the mantle epithelium. Fourteen

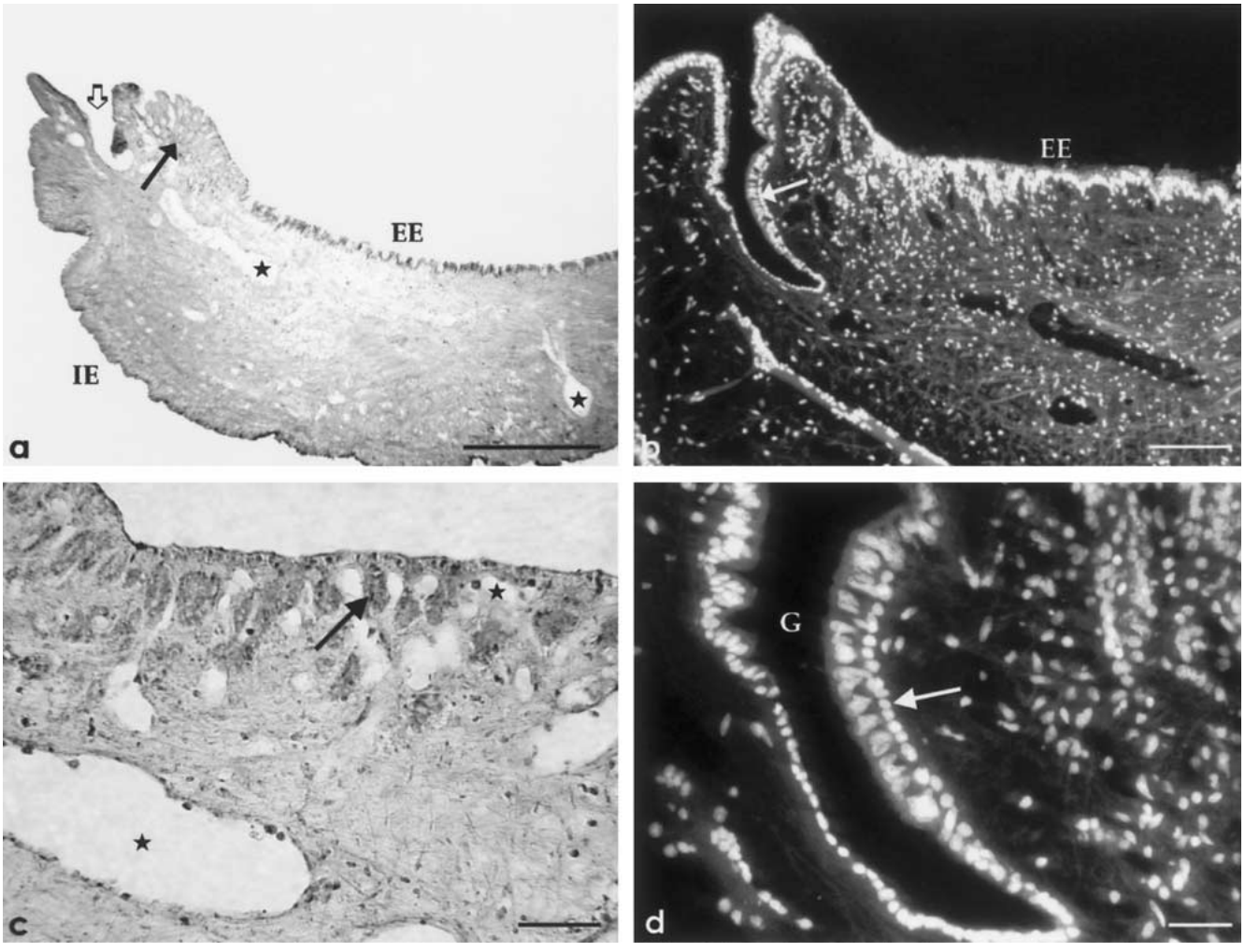

Figure 1. **a**: Light microscopic image showing the structure of the mantle at the shell edge. The periostracal groove (*) makes a boundary between the external epithelium (EE) facing the shell and the inner circumpedal epithelium (IE). The external epithelium appears pleated in its most proximal region, where sheets make a tubular zone (➤) within the connective tissue. The connective layer also contains blood sinuses among connective fibers and muscular bundles. Bar = 500 μm. **b**: Fluorescent microscopy showing the nuclei arrangment in the mantle edge after DAPI reaction. The external epithelium (EE) is monolayered except in the outer fold of the periostracal groove, where 2 layers of nuclei are superimposed, forming a pad (➤) within the groove. Bar = 100 μm. **c**: Detail. Light microscopy of the folded external epithelium. Folding is irregular and sheets can penetrate the connective layer (➤). Blood sinuses are observed in the vicinity of the epithelium, some of them lying close to the bottom of the epithelial cells. Bar = 100 μm. **d**: DAPI fluorescent staining of the bilayered outer fold (➤) of the periostracal groove (G). Bar = 100 μm.

specimens reacted to both MSI 31 and MSI 60 antibodies, and 9 revealed the unique presence of MSI 60–like protein. Samples showing both MSI 31–like and MSI 60–like proteins were spread over the entire time course of the study. Samples with unique MSI 60–like labeling were collected in May.

Our results highlighted 3 zones of MSI 31–like and MSI 60–like protein distribution in the anterior right lobe of the mantle: the pad of outer epithelium in the periostracal groove, the tubular zone, and a limited zone of the folded external epithelium.

MSI 31: Calcitic Matrix Protein

Labeling for MS31–like protein was more or less intensive for the different analyzed specimens. It was distributed in the folded region of the external epithelium (Figure 2, a, d), the tubular zone (Figures 2, c, and 4, b), and the pad of the periostracal groove. Cells of the outer epithelium were generally labeled at their basal and apical poles. Tubular zone cells' labeling was localized within their apical part.

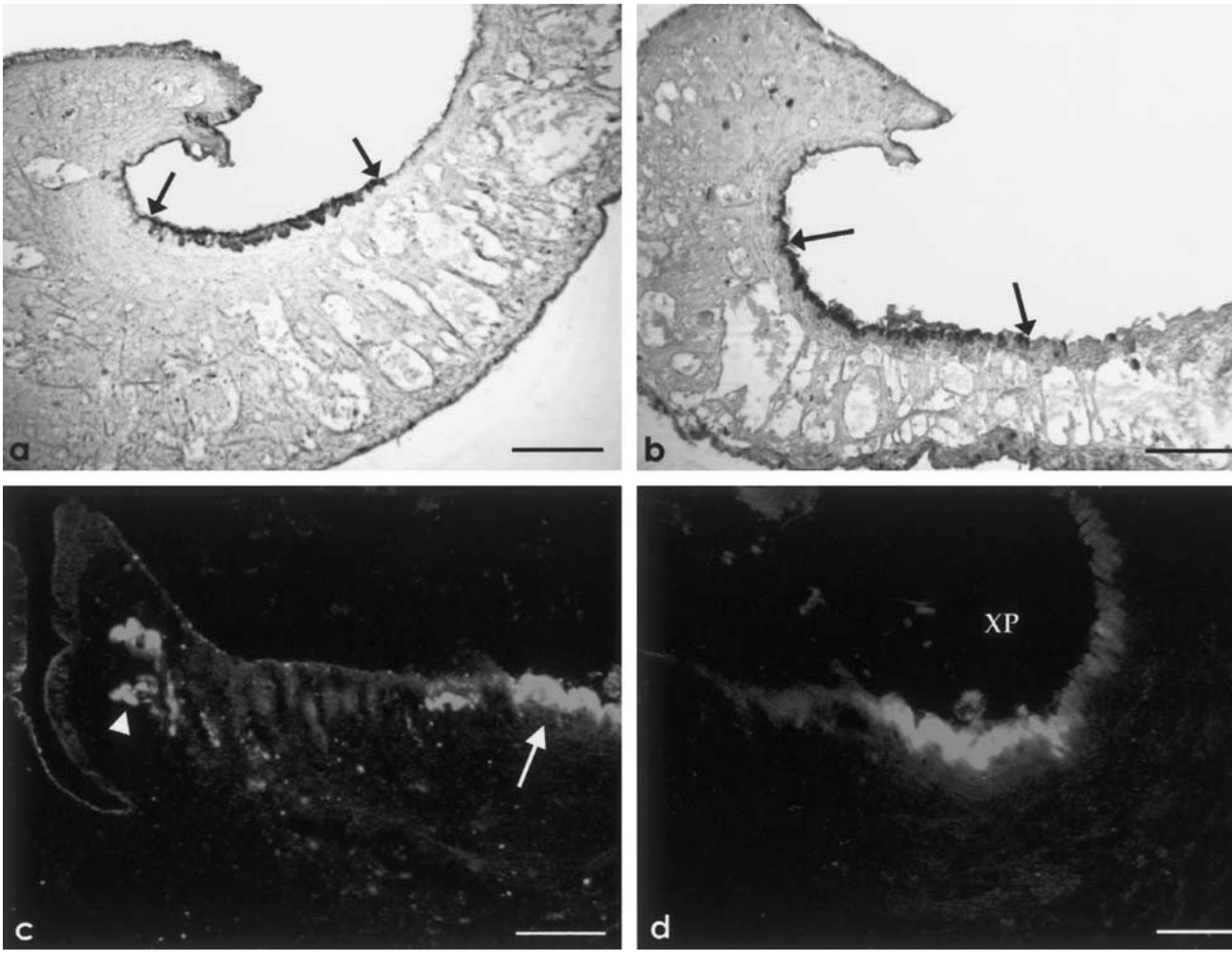

Figure 2. **a**: Light microscopic image showing the zone of MSI 31–like labeling in the pleated external epithelium, in a specimen collected in April (➤). The presence of the protein is revealed by the dark DAB reaction product after immunohistochemical procedure. Bar = 200 μm. **b**: MSI 60–like distribution pattern after immunohistochemistry and DAB labeling (➤) Zonation patterns for MSI 31–like and MSI 60–like shell matrix proteins are quite superimposable. Bar = 200 μm. **c**: Fluorescence microscopy showing MSI 31–like distribution pattern in the foremost part of the mantle edge. Two zones highlight the protein localization: the tubular zone (➢) and the folded external epithelium (➤). Bar = 100 μm. **d**: Zonation of the external epithelium for MSI 31–like protein. Immunofluorescent labeling shows the zonal distribution of the matrix protein in the folded outer epithelium. Extrapallial space (XP). Bar = 200 μm.

MSI 60: Aragonite Matrix Protein

Reaction to MSI 60 antibody was always stronger than to MSI 31 antibody (Figure 3). However, localization of MSI 60–like protein was quite similar to the MSI 31–like protein pattern (Figure 2, a, b; Figure 4, b, c). The specimen collected during the late spring resulted in unique MSI 60–like labeling. The zonation pattern for unique MSI 60–like protein was quite similar to the distribution pattern observed when both MSI 31–like and MSI 60–like proteins were detected.

Miscellaneous

Both MSI 31 and MSI 60 antigens were always localized in the same zones of the epithelium in the analyzed specimen when they were positive to immunochemical reaction (Figure 2, a, b). Our results showed that MS31–like and MSI 60–like proteins were distributed in 3 specific zones of the external epithelium. Two of them, the tubular zone and the folded outer epithelium, were never observed as positive to immunohistochemical reaction at the same time. Although labeling of these 2 regions appeared exclusive, an

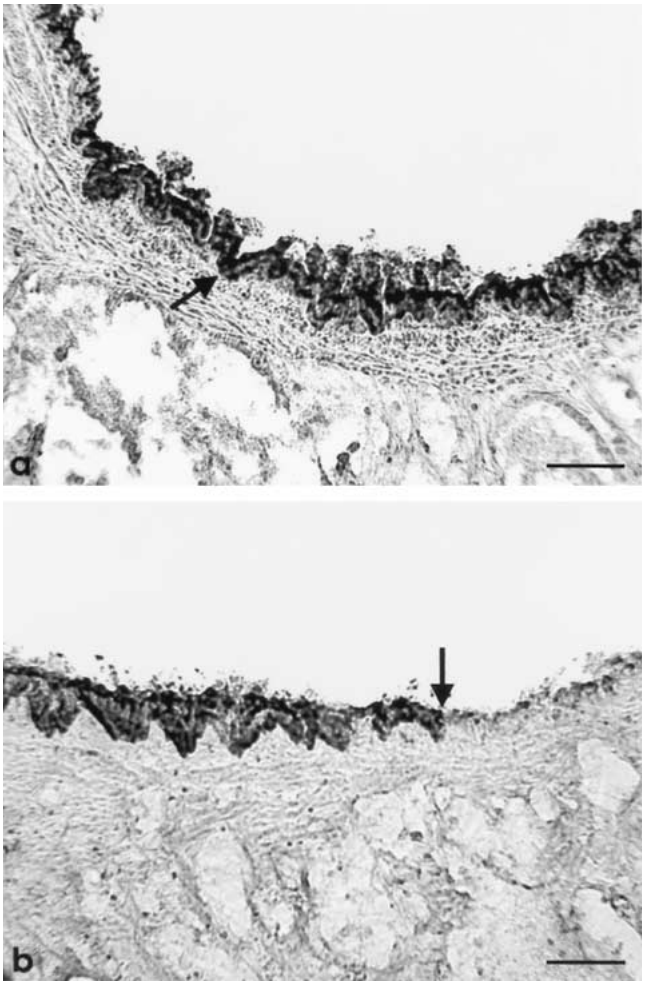

Figure 3. **a**: Light microscopic image of the dark reaction product, signal for MSI 60–like matrix protein (➤), lining the apical and basal poles of the outer epithelial cells. **b**: Abrupt ending (↓) at the distal boundary of the topographic distribution of MSI 60 in the external epithelium. Bar = 50 μm.

alternative pattern was observed during the timecourse of the experiment without apparent sequence order or time period relationship. MSI 60–like protein was still labeled at the late growth cycle period, while MSI 31–like protein was no longer detected within the mantle epithelium. Seven samples collected at the end of April resulted in neither MSI 31–like nor MSI 60–like immunolabeling.

Controls

No immunoreaction was detected in the mantle of the negative control samples or in the mantle of the samples collected during October, the resting period. When positive in animals collected during the growing phase, the labeling was always localized within a restricted zone of the outer

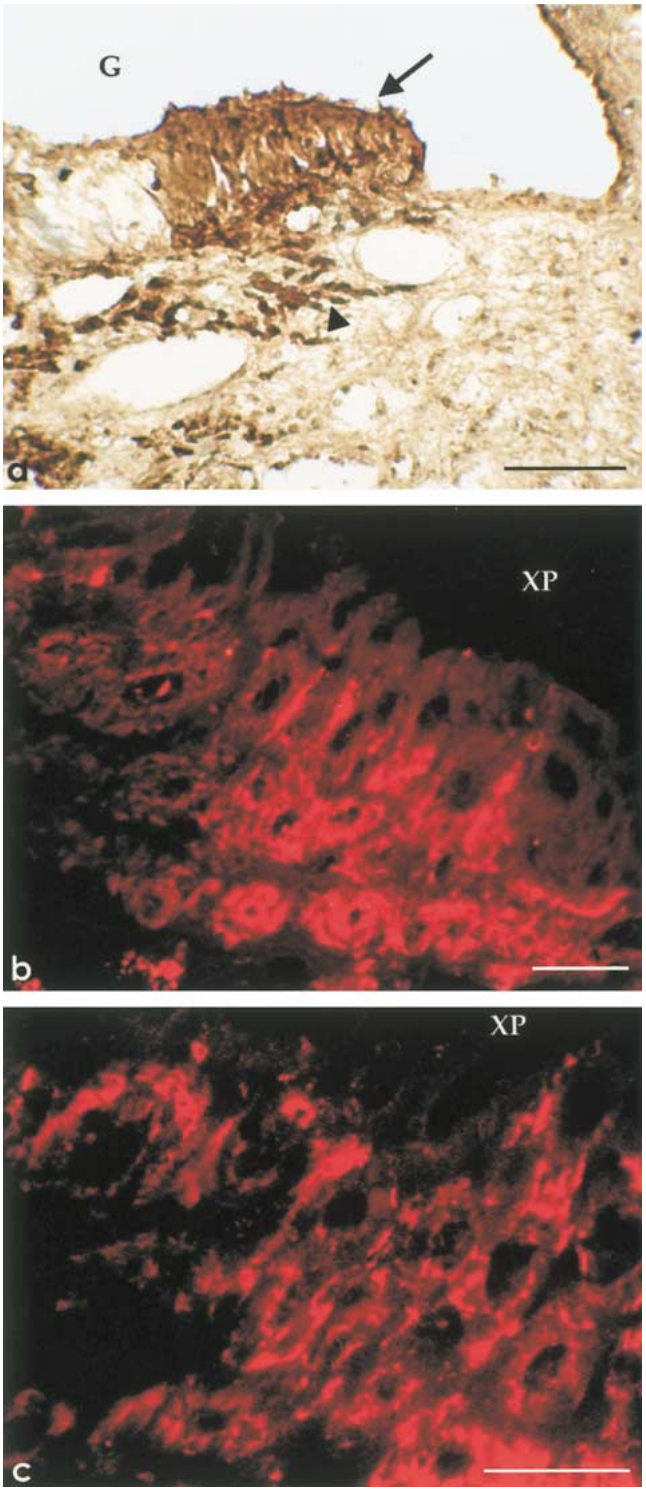

Figure 4. **a**: Immunolabeling of MSI 60–like matrix protein within the pad of epithelial cells (➤) lining the periostracal groove (G). Underneath a cluster of cells belonging to the foremost part of the tubular zone are also labeled (+). Bar = 50 μm. **b,c**: Immunofluorescent labeling showing MSI 31–like (b) and MSI 60–like (c) proteins in the tubular zone of the mantle edge. Extrapallial space (XP). Bar = 50 μm.

mantle epithelium known to be involved in organic shell matrix synthesis, which supports the relevance of the antibodies designed to match shell matrix proteins.

Controls for antibody specificity with the antigen-antibody preincubation step underwent significant fading of the labeling.

The designed antibodies specificity to either MSI 31 or MSI 60 chosen sequences was checked by preincubation of the antibody with the opposite antigen, which resulted in no outcome difference in immunocytochemical reaction when compared with the reaction without preincubation.

Discussion

Haliotis shell contains an inner coverage of nacre, the unique calcium carbonate crystal form being aragonite and a prismatic outer layer where calcium carbonate crystallized under calcite with interspersed aragonite inclusion (Mutvei et al., 1985; Dauphin et al., 1989). The shell is a composite structure, with mineral and organic components, in which acidic peptides and proteins play an important role in achieving crystallization control (Weiner and Hood, 1975). The aim of the present study was to design tools to address zonation in the mantle epithelium and characterize what and when cell populations serve as sources for the shell matrix framework. Therefore we raised antibodies against specific sequences of shell matrix proteins, potentially involved in mineralization control, and looked for the localization of the proteins they match within the mantle epithelium. Sudo et al. (1997) characterized in the shell of *Pinctada* 2 matrix proteins, MSI 31 and MSI 60, specific to the organic matrix of the calcitic and the aragonitic layer, respectively. The peptidic sequences of those proteins were used in this study for specific antibody construction. We chose sequences liable to cause biomineralization.

Previous studies have suggested that protein with $(ASP\text{-}X)_n$ repeating sequence, comprising regular repeating negative charges, could bind Ca^{2+} ion and thus perform an important function in mineralization (Weiner and Hood, 1975; Kono et al., 2000). We can assume that this high content of $(ASP\text{-}X)_n$ repeating sequence could be retrieved in *Haliotis* species. *H. tuberculata* shell matrix proteins contain a high proportion of acidic aminoacids (Albeck et al., 1996; Schäffer et al., 1997; Bédouet et al., 2001). Characterization of shell matrix components, such as nacrein (Miyamoto et al., 1996) and MSI 31 and MSI 60 (Sudo et al., 1997) in *Pinctada*, and mucoperlin (Marin et al., 2000) in *Pina*, showed that those matrix proteins share calcium-binding domains. The sequences that we held were checked for specificity by screening general databanks and selected because of a high ratio of anionic or acidic amino-acid—respectively, 57% and 81% in the designed MSI 31 and MSI 60 sequences. Our work demonstrated the in situ immunolocalization of MSI 31–like and MSI 60–like proteins in outer mantle epithelium of *Haliotis*, liable to be part of the shell matrix proteins pattern. Retrieval of a stain with antibodies run on specific protein from a Bivalvia (*Pinctada*) in a Gastropod (*Haliotis*) highlights the importance of the sequences that we held in the biomineralization process and supports the hypothesis that phylogenic conservation of sequences plays an important role in the control of biomineralization. Lustrin A shares domains with extracellular matrix proteins of bone, teeth, or avian egg shell (Shen et al., 1997); moreover, it has sequence similarity to proteins of the collagen superfamilies and IGFBPs. Weiss et al. (2001) found in perlustrin, a *H. laevigata* (abalone) nacre protein, homologies with insulin-like growth factor binding proteins of vertebrates.

Shell layer production of at least organic matrix has been assigned to the external mantle epithelium. De Waele (1931) first disproved the direct supply of material for shell growth from adjacent mantle cells and proposed a model of shell material deposition from a distant epithelial site involving a maturation step within the extrapalleal fluid. However, little is known about the tissue distribution of the external epithelium with regard to shell matrix protein production.

Northern blot analysis revealed that the dorsal region of the mantle and the mantle edge were the actual sites for shell matrix protein encoding (Miyamoto et al., 1996; Kono, 2000). Sudo et al. (1997) reported in situ hybridization results showing the limited region in which the mantle expressed 2 shell-specific matrix proteins, MSI 31 and MSI 60 messengerRNA in Pinctada. The two regions are contiguous and exclusive—MSI 30 being expressed within a more external area at the mantle edge, and MSI 60 in the adjacent folded external epithelium.

We obtained a similar pattern of expression of these proteins in *Haliotis* with a complete overlap of the 2 zones described in Pinctada. Bivalvia and Gastropoda are both conchiferan mollusks and thus share a triplicate mantle edge. The presence of more apparent folds in *Pinctada*, interpreted as a subdivision of the *Haliotis* pattern (Schäffer et al., 1997), may also reflect a separation of cell populations secreting shell matrix proteins in 2 separate zones in *Haliotis* mantle.

It is believed that the mantle edge is involved in prismatic layer ingrowth, and the whole mantle surface in the thickening of the nacreous layer (Timmermans, 1969; Saleuddin, 1976). Our work was designed to map shell matrix protein production within the growth cycle (Clavier and Richard, 1985), and our results showed 2 period-related patterns. Particular to *Haliotis* is the composition of the prismatic outer layer, which consists of a mix of aragonite and calcite (Mutvei et al., 1985; Dauphin et al., 1989). The original dual crystallography of the external layer of the shell in *Haliotis* with the 2 polymorphs supports our finding that cell clusters in the front edge of the mantle could be able to synthesize both aragonite and calcite matrix proteins. The labeling of unique MSI 60–like protein in the late spring samples argues in favor of the specificity of the designed MSI 60 antibody to match aragonitic matrix protein. We could distinguish 2 phases in shell matrix synthesis within the mantle: a first period lasting almost the entire time of our study, during which both aragonite and calcite matrix synthesis occur, involving the outer prismatic layer ingrowth, but possibly nacreous layer ingrowth too, and a final short period, when only material for the thickening of the inner nacreous layer is produced. This latter period lasts until the end of the annual growing cycle, and some samples collected at this time totally lacked MSI labeling, as did animals collected during the autumnal resting period. The detection of unique MSI 60–like protein later during the growth cycle is consistent with this timetable. This process is underlined by a switch in the shell matrix protein synthesis from the mantle cells.

Earlier work indicated that aragonite and calcite were deposited in the prismatic layer, either simultaneously or by rapid changes in mineralization under the control of mantle epithelium cells (Mutvei et al., 1985; Dauphin et al., 1989). Hawkes et al., (1996) also observed in *Haliotis rubra* that across the prismatic layer, calcite and aragonite were deposited simultaneously, but also showed that the mineralization on surface terraces can change from calcite to aragonite or vice versa within shorts periods. Indeed, Belcher et al. (1996) found in vitro that a similarly abrupt calcite-to-aragonite transition was induced during the growth of calcite crystals by the addition of water-soluble, polyanionic proteins isolated from the aragonitic nacre of *H. rufescens*. This raises the question of what variations can modify the functioning of the pallial epithelium within an area where shell microstructural units grow (Belcher et al., 1996; Thompson et al., 2000). The ability of *Haliotis*, especially in species with mixed mineralogic structure), to invert locally the nature of the skeletal mineral, which leads to formation of inclusions of one mineral within the other (Mutvei et al., 1985; Dauphin et al., 1989), raises the issue of the amplitude of the corresponding changes in the synthesis secretion and regulation of the organic matrix that govern this phenomenon. Our results highlighted the pallial epithelium's ability to secrete the 2 specific peptidic matrices synchronously, which leads to a local inversion, at the shell edge, of the mineralogic nature of the crystals deposited during the growth cycles.

The sharp phase transition may involve an inhibitor of calcite growth and growth acceleration for aragonite. This points to an underlying genetic switch controlling organic matrix secretion. A precedent for such a control is seen in the abrupt transition from the larval to the adult abalone shell at metamorphosis. The process is accompanied by a switch in production of polyanionic proteins controlling shell biomineralization (Belcher et al., 1996). Moreover, Fritz et al. (1994) pointed out that the nacre-secreting cells are able to be involved in calcitic deposition and suggested that epithelial cells may respond to a downregulation of nacreous matrix production until the calcite protein matrix is established. Molluscan shell architecture results from a dynamic interaction via extrapallial fluid between the cell and the mineral interface in which cell recognition of the mineral surface governs a genetic switch controlling the matrices, production and, thus, the structure of the mineral. Previous work had demonstrated by means of in vivo and in vitro experiments that soluble signals enclosed in nacre matrix can diffuse through the surrounding media and induce cell activation (Lopez et al., 1992, 1994; Atlan et al., 1997, 1999; Sud et al., 2001). The authors established that nacre matrix gathered water-soluble factors activating cells involved in the biomineralization process, and was also potent in influencing differentiation of mesenchymal cells or stem cells into biomineralizing lineage cells in a vertebrate model (Lamghari et al., 1999; Almeida et al.; 2000; Moutahir-Belqasmi et al., 2001).

This led to the essential interfacial role played by the extrapallial space as a diffusion chamber where microstructural units generate compartmentation. Little is known about how newly secreted matrix materials assemble into a functioning, precisely arranged network, capable of directing and controlling the construction of mineral formations with precise details. Insoluble proteins can bring about a first 3-dimensional lattice modulating the stereotaxical position of carbonate group template for nucleation (Feng et al., 2000; Hattan et al., 2001). Sharper crystalli-

zation control may involve a joint venture with soluble matrix components. Shell matrix proteins generally show plurifunctionalities such as structural properties, binding, or enzymatic activities, associated with calcium binding or inhibition from protein degradation (Miyamoto et al., 1996; Shen et al., 1997).

One can suppose that growth-regulating mechanisms occur directly in the extrapallial space, the epithelial cells supplying the puzzling material.

Our model established that histologic changes in the pallial structure seem to be associated with shell matrix production. Inside the mantle edge, the tubular zone and the adjacent outer epithelium organization changed. When the shell matrix proteins appeared localized at both apical and basal parts of the epithelial cells, numerous large blood sinuses were observed at the bottom of the epithelium, allowing local exchange of a factor implicated in the control of the mineralization process. Epithelial cells of the mantle are the main cell type involved in the shell mineralization in which regulation can occur. Cell culture, and especially co-cultures of epitheliocytes and hemocytes, can provide tools to investigate the conditions for epithelial cell plasticity (Sud et al., 2000). Our work designed a specific zone for shell matrix production, but we must keep in mind that shell damage can induce a cellular wake-up elsewhere in the outer epithelium (Wilbur, 1964; Samata et al., 1999).

In *Haliotis*, plasticity appears in epithelial secreting cells according to their cyclic activity; these direct the supply of disposable matrix material on a precise timetable. This endogenous rhythm of functional zones of the epithelium can be the result of a combined response to physiologic inducing factors from the mollusk soft body and to local inducers provided by the shell itself.

Further investigations are needed to determine whether the external epithelium is a mosaic of zonal matrix molecules producing cell populations, or if the zone described here is the controlling one for all components of the shell matrix. We will focus on this zonation in an attempt to elucidate the schedule of matrix component production.

Acknowledgments

The authors thank SMEL (Syndicat Mixte de 1'Equipement du Littoral, Blainville sur mer, France) for supplying the animals according to our requirements. Thanks are also due to Mrs. Francine Lallier for editing the text.

References

Albeck, S., Weiner, S., and Addadi, L. (1996). Polysaccharides of intracrystalline glycoproteins modulate calcite crystal growth in vitro. *Chem Eur J* 2:278–284.

Almeida, M.J., Milet, C., Peduzzi, J., Pereira, L., Haigle, J., Barthelemy, M., and Lopez, E. (2000). Effect of water-soluble matrix fraction extracted from the nacre of *Pinctada maxima* on the alkaline phosphatase activity of cultured fibroblasts. *J Exp Zool (Mol Dev Evol)* 288:327–334.

Atlan, G., Balmain, N., Berland, S., Vidal, B., and Lopez, E. (1997). Reconstruction of human maxillary defects with nacre powder: histological evidence for bone regeneration. *C R Acad Sci (Série III: Sciences de la vie)* 320:253–258.

Atlan, G., Delattre, O., Berland, S., Le Faou, A., Nabias, G., Cot, D., and Lopez, E. (1999). Interface between bone and nacre implants in sheep. *Biomaterials* 20:1017–1022.

Bedouet, L., Schuller, M.J., Marin, F., Milet, C., Lopez, E., and Giraud, M. (2001). Soluble proteins of the nacre of the giant oyster *Pinctada maxima* and of the abalone *Haliotis tuberculata*: extraction and partial analysis of nacre proteins. *Comp Biochem Physiol* 128:389–400.

Belcher, A.M., Wu, X.H., Christensen, R.J., Hansma, P.K., Stucky, G.D., and Morse, D.E. (1996). Control of crystal phase switching and orientation by soluble mollusc-shell proteins. *Nature* 381:56–58.

Bielefeld, U., Körtje, K.H., Rahmann, H., and Becker, W. (1993). The shell-forming mantle epithelium of *Biomphalaria glabrata* (Pulmonata): ultrastructure, permeability and cytochemistry. *J Molluscan Stud* 59:323–338.

Clavier J., and Richard O. (1985). Etude sur les ormeaux dans la région de Saint-Malo. Association pour la mise en valeur du littoral de la côte d'Emeraude.

Crenshaw, M.A. (1972). The soluble matrix from *Mercenaria mercenaria* shell. *Biomineralisation* 6:6–11.

Dauphin, Y., Cuif, J.P., Mutvei, H., and Denis, A. (1989). Mineralogy, chemistry and ultrastructure of the external shell-layer in ten species of *Haliotis* with reference to *Haliotis tuberculata* (Mollusca: *Archaeogastropoda*). *Bull Geol Inst Univ Uppsala NS* 15:7–38.

De Waele, A. (1930). In: *Mem Acad Roy de Belgique*, classe des Sciences, t.X, pp 31–51.

Falini, G., Albeck, S., Weiner, S., and Addadi, L. (1996). Control of aragonite or calcite polymorphism by mollusk shell macromolecules. *Science* 271:67–69.

Feng, Q.L., Pu, G., Pei, Y., Cui, F.Z., Li, H.D., and Kim, T.N. (2000). Polymorph and morphology of calcium carbonate crystals

induced by proteins extracted from mollusk shell. *J Cryst Growth* 216:459–465.

Fritz, M., Belcher, A.M., Radmacher, M., Walters, G.D., Hansma, P.K., Stucky, G.D., Morse, D.E., and Mann, S. (1994). Flat pearls from biofabrication of organized composites on inorganic substrates. *Nature* 371:49–51.

Garaerts, W.P.M. (1976). Control of growth by the neuro-secretory hormone of the light green cells of the freshwater snail *Lymnea stagnalis*. *Gen Comp Endocrinol* 29:61–71.

Hattan, S.J., Laue, T.M., and Chasteen, N.D. (2001). Purification and characterization of a novel calcium-binding protein from the extrapallial fluid of the mollusc, *Mytilus edulis*. *J Biol Chem* 276(6):4461–4468.

Hawkes, G.P., Day, R.W., Wallace, M.W., Nugent, K.W., Bettiol, A.A., Jamieson, D.N., and Williams, M.C. (1996). Analyzing the growth and form of mollusc shell layers, *in situ*, by cathodoluminescence microscopy and Raman spectroscopy. *J Shellfish Res* 15(3):659–666.

Kobayashi, I. (1973). Data on the differential thermal analyses of bivalvian shells. *Bull Fossil Club Tokyo* 7:1–4.

Kono, M., Hayashi, N., and Samata, T. (2000). Molecular mechanisms of the nacreous layer formation in *Pinctada maxima*. *Biochem Biophys Res Commun* 264:213–218.

Lamghari, M., Almeida, M.J., Berland, S., Huet, H., Laurent, A., Milet, C., and Lopez, E. (1999). Stimulation of bone marrow cells and bone formation by nacre: *in vivo* and *in vitro* studies. *Bone* 25:91S–94S.

Lopez, E., Vidal, B., Berland, S., Camprasse, S., Camprasse, G., and Silve, C. (1992). Demonstration of the capacity of nacre to induce bone formation by human osteoblasts maintened *in vitro*. *Tissue Cell* 24:667–679.

Lopez, E., Berland, S., and Le Faou, A. (1994). Nacre, osteogenic and osteoinductive properties. *Bull Inst Ocean Monaco* 14:49–57.

Marin, F., Corstjens, P., de Gaulejac, B., De Vrind Jong, E., and Westbroek, P. (2000). Mucins and molluscan calcification: molecular characterization of mucoperlin, a novel mucin-like protein from the nacreous shell layer of the fan mussel *Pinna nobilis* (Bivalvia, Pteriomorpha). *J Biol Chem* 275(27):20667–20675.

Miyamoto, H., Miyashita, T., Okushima, M., Nakano, S., Morita, T., and Matsushiro, A. (1996). A carbonic anhydrase from the nacreous layer in oyster pearls. *Proc Natl Acad Sci USA* 93:9657–9660.

Moutahir-Belqasmi, F., Balmain, N., Lieberrher, M., Borzeix, S., Berland, S., Barthelemy, M., Pedduzi, J., Milet, C., and Lopez, E. (2001). Effect of water soluble extract of nacre (*Pinctada maxima*) on alkaline phosphatase activity and Bcl-2 expression in primary cultured osteoblasts from neonatal rat calvaria. *J Mater Sci Mater Med* 12(1):1–6.

Mutvei, H., Dauphin, Y., and Cuif, J.P. (1985). Observations sur l'organisation de la couche externe du test des *Haliotis* (Gastropoda): un cas exceptionnel de la variabilité minéralogique et microstructurale. *Bull Mus Nat Hist Nat Paris Ser 4* 7(1):73–91.

Nakahara, H., Kakei, M., and Bevelander, G. (1981). Studies on the formation of the crossed lamellar structure in the shell of *Strombus gigas*. *Veliger* 23(3):207–211.

Saleuddin, A.S.M. (1975). An electron microscopic study on the formation of the periostracum in *Helisoma* (Mollusca). *Calc Tiss Res* 18:297–310.

Saleuddin, A.S.M. (1976). Ultrastructural studies on the structure and formation of the periostracum in Helisoma (Mollusca). In: *The Mechanisms of Mineralization in the Invertebrates and Plants*, Watabe, N. (eds). University of South Carolina Press pp 309–337.

Samata, T. (1990). Ca-binding glycoproteins in molluscan shells with different types of ultrastructure. *Veliger* 33(2):190–201.

Samata, T., Hayashi, N., Kono, M., Hasegawa, K., Horita, C., and Akera, S. (1999). A new matrix protein family related to the nacreous layer formation of *Pinctada fucata*. *FEBS* 462:225–229.

Schäffer, T.E., Ionesco-Zanetti, C., Proksch, R., Fritz, M., Walters, D.A., Almqvist, N., Zaremba, C.M., Belcher, A.M., Smith, B.L., Stucky, G.D., Morse, D.E., and Hansma, P.K. (1997). Does abalone nacre form by heteroepitaxial nucleation or by growth trough mineral bridges? *Chem Mater* 9:1731–1740.

Shen, X., Belcher, A.M., Hansma, P.K., Stucky, G.D., and Morse, D.E. (1997). Molecular cloning and characterization of lustrin A, a matrix protein from shell and pearl nacre of *Haliotis rufescens*. *J Biol Chem* 272(51):32472–32481.

Simkiss, K., and Wilbur, K.M. (1987). Molluscs—epithelial control of matrix and minerals. In: *Biomineralization: Cell Biology and Mineral Deposition*, Simkiss, K., and Wilbur, K.M. (eds). New york, N.Y.: Academic Press Inc., pp 230–260.

Sud, D., Auzoux-Bordenave, M., Martin, M., and Doumenc, D. (1998). Cell cultures from the abalone *Haliotis tuberculata*: a new tool for in vitro study of biomineralization. In: *New Developments in Marine Biotechnology*, Le Gal and Halverson (eds). New York, N,Y.: Plenum Press, pp 165–170.

Sud, D., Doumenc, D., Lopez, E., and Milet, C. (2001). Role of water-soluble matrix fraction, extracted from the nacre of *Pinctada maxima*, in the regulation of cell activity in abalone mantle cell culture (*Haliotis tuberculata*). *Tissue Cell* 33(2):154–160.

Sudo, S., Fujikawa, T., Nagakura, T., Ohkubo, T., Sakaguchi, K., Tanaka, M., Nakhashima, K., and Takahashi, T. (1997). Structures of mollusc shell framework proteins. *Nature* 387:563–564.

Thompson, J.B., Paloczi, G.T., Kindt, J.H., Michenfelder, M., Smith, B.L., Stucky, G.D., Morse, D.E., and Hansma, P.K (2000). Direct observation of the transition from calcite to aragonite growth as induced by abalone shell proteins. *Biophysics* 79:3307–3312.

Timmermans, L.P.M. (1969). Studies on shell formation in molluscs. *Neth J Zool* 19:417–523.

Weiner, S., and Hood, L. (1975). Soluble protein of the organic matrix of mollusk shells: a potential template for shell formation. *Science* 190:987–989.

Weiner, S., and Traub, M. (1984). Macromolecules in mollusc shells and their functions in biomineralization. *Phil Trans R Soc Lond B* 304:425–434.

Weiss, I.M., Kaufmann, S., Mann, K., and Fritz, M. (2000). Purification and characterization of perlucin and perlustrin, two new proteins from the shell of the mollusc *Haliotis laevigata*. *Biochem Biophys Res Commun* 267:17–21.

Weiss, I.M., Göhring, W., Fritz, M., and Mann, K. (2001). Perlustrin, a *Haliotis laevigata* (abalone) nacre protein, is homologous to the insuline-like growth factor binding protein N-terminal module of verebrates. *Biochem Biophys Res Commun* 285:244–249.

Wilbur, K.M. (1964). Shell formation and regeneration. In: *Physiology of Mollusca*, Wilbur, K.M., and Yonge, C.M. (eds). New york, N.Y.: Academic Press, pp 243–282.

Zaremba, C.M., Belcher, A.M., Fritz, M., Li, Y., Mann, S., Hansma, P.K., Morse, D.E., Speck, J.S., and Stucky, G.D. (1996). Critical transitions in the biofabrication of abalone shells and flat pearls. *Chem Mater* 8(3):679–690.